

Critically coupled resonators in vertical geometry using a planar mirror and a 5 nm thick absorbing film

Jonathan R. Tischler, M. Scott Bradley, and Vladimir Bulović

Department of Electrical Engineering and Computer Science, Massachusetts Institute of Technology, Cambridge, Massachusetts 02139

Received March 3, 2006; revised March 27, 2006; accepted April 1, 2006; posted April 10, 2006 (Doc. ID 68646)

A (5.1 ± 0.5) nm thick film of high oscillator strength J-aggregated dye critically couples to a single dielectric mirror, absorbing more than 97% of incident $\lambda = 591$ nm wavelength light, corresponding to an effective absorption coefficient of $(6.9 \pm 0.7) \times 10^6 \text{ cm}^{-1}$ for (film thickness)/ $\lambda < 1\%$. © 2006 Optical Society of America
OCIS codes: 230.5750, 310.1210.

We report the linear optical properties of a critically coupled resonator (CCR), a thin-film structure that can absorb nearly all of the incident light of a given wavelength in a few-nanometer-thick absorbing film. The CCR, sketched in Fig. 1, consists of a dielectric Bragg reflector (DBR) as the mirror, a (5.1 ± 0.5) nm thick film of organic material as the absorbing layer, and a spacer layer of transparent material that separates the mirror and absorber layer by the correct distance needed for critical coupling. When light of wavelength $\lambda_c = 591$ nm is incident on the CCR of Fig. 1 from the absorber layer side of the device, the measured reflectance is $R = 2\%$ (Fig. 2). In contrast, for the DBR with the spacer but without the absorbing layer, the reflectance at $\lambda_c = 591$ nm exceeds 95%, showing the dramatic change due to critical coupling. A similar structure has been discussed in the context of microwave engineering to eliminate wave reflections from conducting surfaces.¹ For the same CCR the transmittance at λ_c is $T = 1\%$. Consequently, 97% of the incident light is absorbed within the (5.1 ± 0.5) nm thick absorber layer, corresponding to a peak effective absorption coefficient of $\alpha_{\text{eff}} = (6.9 \pm 0.7) \times 10^6 \text{ cm}^{-1}$.

In the CCR of Fig. 1, the absorbing thin film consists of layers of the cationic polyelectrolyte PDAC (poly diallyldimethylammonium chloride) and J aggregates of the anionic cyanine dye TDBC (5,6-dichloro-2-[3-[5,6-dichloro-1-ethyl-3-(3-sulfopropyl)-2(3H)-benzimidazolidenel]-1-propenyl]-1-ethyl-3-(3-sulfopropyl) benzimidazolium hydroxide, inner salt, sodium salt), molecular structures shown in Fig. 1. J aggregates are crystallites of dye in which the transition dipoles of the constituent molecules strongly couple to form a collective narrow-linewidth optical transition possessing oscillator strength derived from all the aggregated molecules.² Neat films of PDAC/TDBC contain a high density of J-aggregated TDBC and therefore have the high peak absorption coefficient of $\alpha = 1.0 \times 10^6 \text{ cm}^{-1}$.³

A wavelength-resolved T -matrix simulation⁴ (Figs. 3 and 4) numerically confirms the experimentally observed critical coupling phenomenon. To simulate the CCR's reflectance, we first constructed T matrices corresponding to the PDAC/TDBC film and the DBR.

For the PDAC/TDBC film, with thickness $d_a = 5.1$ nm, the real and imaginary components of the refractive index ($n + j\kappa = \tilde{n}$) were obtained via a Kramers–Kronig regression of the neat film reflectance data, which as shown in Fig. 3 reproduces the neat film transmittance spectrum.³ The DBR was modeled as consisting of 8.5 pairs of TiO_2 and Al_2O_3 layers, with refractive indices of $n = 2.39$ and $n = 1.62$, respectively, with the layer thickness adjusted to satisfy the Bragg condition ($d_i = \lambda/4n_i$) for $\lambda = 565$ nm. We combined these models with a model of the spacer layer with $n_s = 1.62$ and thickness d_s left as a free parameter. The simulation reproduces critical coupling at $\lambda_c = 591$ nm (Fig. 4) for a spacer layer thickness $d_s = 90$ nm and odd multiples thereof. When d_s is set to a value greater or less than 90 nm, critical coupling does not occur at another wavelength.

Critical coupling occurs when (1) all of the incident optical power is transferred through the front face of the CCR absorber layer and (2) the Poynting vector in the dielectric layers is purely imaginary. Conse-

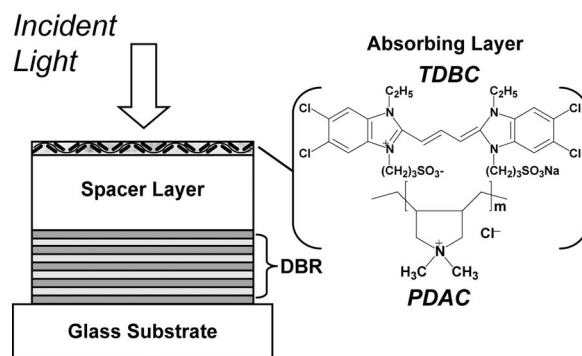


Fig. 1. Critically coupled resonator (CCR) structure. The device consists of a dielectric Bragg reflector (DBR), a transparent spacer layer, and a layer of J-aggregate cyanine dye. The DBR consists of 8.5 pairs of sputter-coated TiO_2 and Al_2O_3 layers, ending on TiO_2 . The spacer layer is an additional sputter-coated layer of Al_2O_3 . The J-aggregate layer consists of the cationic polyelectrolyte PDAC and the anionic cyanine dye TDBC deposited via sequential immersion into cationic and anionic aqueous solutions (pH=5.5) utilizing the technique described in Ref. 3. Reflection and transmission measurements are made with light incident from the J-aggregate side of the device.

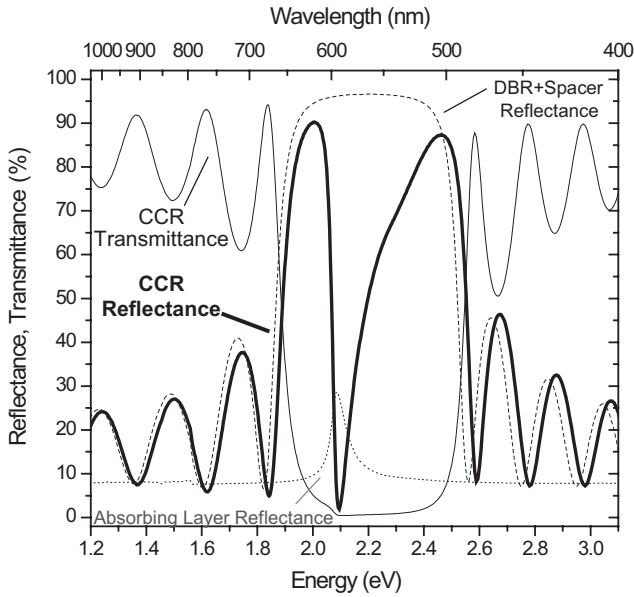


Fig. 2. Measured reflectance and transmittance for the CCR with $d_s = (90 \pm 1)$ nm, along with reflectance data for the neat PDAC/TDBC film and for the dielectric stack consisting of DBR with spacer layer. At $\lambda_c = 591$ nm, the CCR absorbs 97% of the incident light.

quently, two boundary conditions must be simultaneously satisfied to achieve critical coupling: that is, the magnitude of the reflection coefficient from air to the absorber layer front face must be zero, and the magnitude of the reflection coefficient from the absorber layer back face to the dielectric spacer must be unity. The first condition is realized by impedance matching the CCR with air, and the second by mismatching the impedances across the absorber–spacer interface by a phase difference of $\pm\pi/2$. The second boundary condition also dictates that the Poynting vector is purely real on the absorber layer side of the interface.

The critical coupling phenomenon observed for the 5.1 nm thick film of PDAC/TDBC spaced 90 nm from the DBR of Fig. 1 applies more generally to any thin film absorber layer of sufficient oscillator strength (i.e., κ), providing d_a and d_s are set to the appropriate thicknesses. To demonstrate this, we constructed a generalized formalism of critical coupling for the CCR structure of Fig. 1. To simplify the analysis, we assume that the mirror is a single layer of metal that is thick enough to neglect reflections from the mirror–substrate interface. The structure of Fig. 1 then reduces to four regions of different refractive index; 1, air; 2, the absorber layer; 3, the spacer layer; and, 4, the Ag mirror. These have three interfaces: 1–2, 2–3, and 3–4, with thicknesses for absorber and spacer layers, d_a and d_s , represented as L_2 and L_3 , respectively. The reflection coefficient, r , of the structure for normal-incidence light is given by

$$r = [r_{12}(1 + r_{23}r_{34}e^{2j\beta_3L_3}) + e^{2j\beta_2L_2}(r_{23} + r_{34}e^{2j\beta_3L_3})] / [(1 + r_{23}r_{34}e^{2j\beta_3L_3}) + r_{12}e^{2j\beta_2L_2}(r_{23} + r_{34}e^{2j\beta_3L_3})], \quad (1)$$

where $r_{ij} = (\tilde{n}_i - \tilde{n}_j) / (\tilde{n}_i + \tilde{n}_j)$ and $\beta_i = 2\pi\tilde{n}_i/\lambda$ are the Fresnel coefficient for the interface ij and the wave

vector for the i th layer, respectively. The percent reflectance, R , is given by $R = |r|^2$. Critical coupling occurs when parameters are chosen such that $R = 0\%$, since no light is transmitted through the CCR.

Figure 5 shows the absorber and spacer layer thicknesses that are needed to achieve critical coupling as a function of the absorber layer κ . The result is plotted for three different values of the real part of the absorber layer refractive index, $n_a \in (1.55, 1.75, 2.0)$, $n_s = 1.7$ throughout, and the single mirror layer is assumed to be Ag, with complex refractive index⁵ $\tilde{n} = 0.259 + j3.887$ at $\lambda = 584$ nm. The

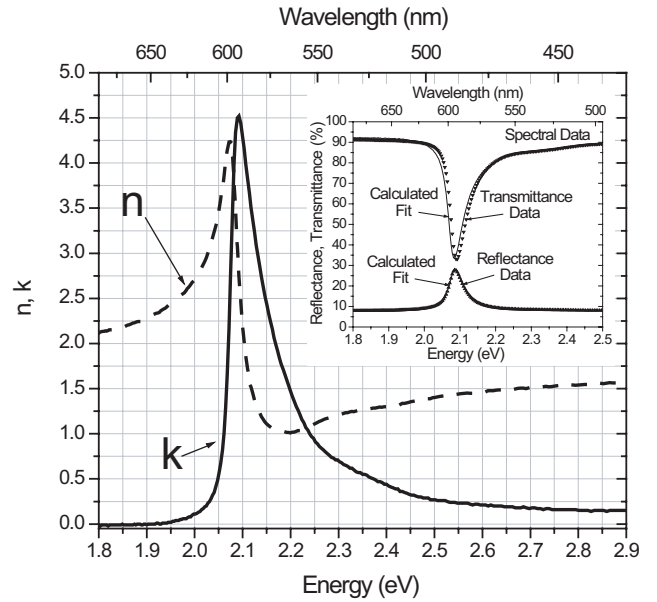


Fig. 3. Spectrally resolved real and imaginary components of the refractive index, (n, κ) , for a 5.1 ± 0.5 nm thick PDAC/TDBC film deposited on an SiO_2 substrate.³ Inset, spectral data with fits calculated from (n, κ) values. κ peaks at $\lambda = 593$ nm, while reflectance peaks at $\lambda = 595$ nm.

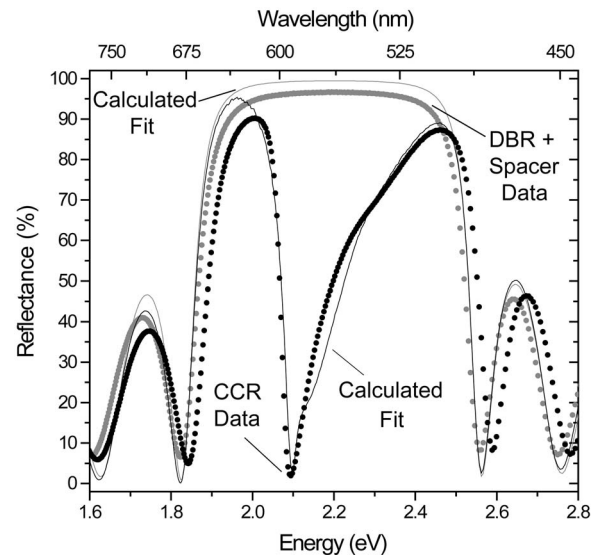


Fig. 4. Measured and calculated reflectance for the CCR device and DBR spacer stack. The calculated reflectance is based on the T -matrix formalism described in the text. The calculated fit matches the experimentally observed reflectance minimum at $\lambda_c = 591$ nm.

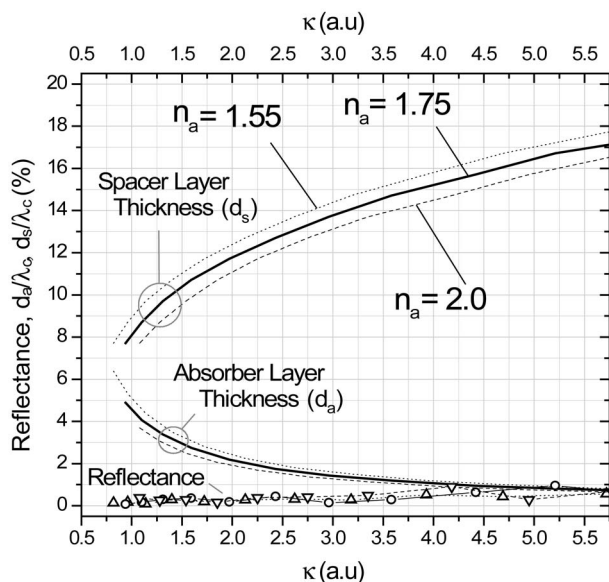


Fig. 5. Generalized formalism for critically coupling absorber layer of Fig. 1 as a function of absorber κ . Thicknesses for absorber and spacer layers are normalized to the CCR wavelength, λ_c . The reflectance plotted is at λ_c . For the spacer layer $n_s=1.7$, and for the absorber the real component of the refractive index is set to $n_a \in (1.55, 1.75, 2.0)$.

thicknesses are normalized to λ_c to emphasize the generality of this model. The model shows that as κ increases, the absorber layer thickness must decrease to satisfy CCR conditions, with a corresponding increase in the spacer layer thickness. It also shows that for a given κ , as n_a increases, d_s decreases, as expected, while d_a remains nearly constant. The model dictates that in order to critically couple the $d_a=5.1$ nm thick PDAC/TDBC film of Fig. 1 at $\lambda_c=584$ nm ($d_a/\lambda_c=0.87\%$) the extinction coefficient of the film must be $\kappa=4.2$, which also sets $d_s/\lambda_c=15\%$ or, equivalently, $d_s=88$ nm for $n_a=2.0$ and $n_s=1.7$. These theoretical values agree well with the experimentally measured $\kappa=4.2$ and $n_a=2.1$ at 591 nm (from Fig. 3) and $d_s=90$ nm for the CCR structure in Fig. 2 with $n_s=1.62$.

Looking beyond films of PDAC/TDBC and other J aggregates, we can envisage building CCR's with a variety of highly absorptive materials. Among non-epitaxially grown materials, CCR structures could be implemented with organic polymers that are used in biological assays and chemical sensors, with molecular materials used in photodetectors and xerographic photoresistors, and in the emerging uses of collo-

idally grown inorganic nanocrystal quantum dots (QDs), with the QD continuum states providing the necessary absorption.⁶

If the absorbing films that satisfy the critical coupling conditions of Fig. 5 were deposited on glass ($n=1.48$) as neat films, T-matrix simulation shows that at λ_c they would absorb 32% of the incident light. The absorption gain from the CCR is therefore a factor of 3.1. Thus the CCR is essential for maximizing light absorption in a nanometer-scale thin-film single-mirror vertical geometry structure.

Finally, the CCR can be viewed as an integral part of recently demonstrated microcavity structures that exhibit strong coupling of light and matter in the form of exciton-polariton resonances,⁷ wherein PDAC/TDBC films were placed at the antinode of the microcavity's optical field. Conceptually, these structures are a CCR plus a top mirror that is separated approximately $\lambda/4$ away from the PDAC/TDBC absorber film of the CCR. Measurement of the polaritonic bandgap observed as a high reflectance band centered around the uncoupled exciton resonance follows naturally, since with the CCR in place there is no optical feedback from the bottom mirror to cause a resonant dip in reflectance in this wavelength band. Thus an understanding of the CCR phenomenon can also assist in the development of future devices that operate in the strong coupling regime.

The authors thank Arto Nurmikko and his research group, the Defense Advanced Research Projects Agency Brown University Optocenter, and The MIT MRSEC Program of the National Science Foundation for support. J. Tischler's e-mail address is jrt@mit.edu.

References

1. S. Ramo, J. R. Whinnery, and T. Van Duzer, *Fields and Waves in Communication Electronics* (Wiley, 1984), p. 287.
2. M. Vanburgel, D. A. Wiersma, and K. Duppen, *J. Chem. Phys.* **102**, 20 (1995).
3. M. S. Bradley, J. R. Tischler, and V. Bulović, *Adv. Mater.* (Weinheim, Germany) **17**, 1881 (2005).
4. L. A. Coldren and S. W. Corzine, *Diode Lasers, and Photonic Integrated Circuits* (Wiley, 1995), p. 74.
5. The refractive index of Ag at $\lambda=584$ nm is derived from a fit to the \tilde{n} data published in H. J. Hagemann, W. Gudat, and C. Kunz, *J. Opt. Soc. Am.* **65**, 742 (1975).
6. C. A. Leatherdale, W.-K. Woo, F. V. Mikulec, and M. G. Bawendi, *J. Chem. Phys.* **106**, 7619 (2002).
7. J. R. Tischler, M. S. Bradley, V. Bulović, J. H. Song, and A. Nurmikko, *Phys. Rev. Lett.* **95**, 036401 (2005).